ORIGINAL RESEARCH

Silver nanoparticles outperform gold nanoparticles in radiosensitizing U251 cells in vitro and in an intracranial mouse model of glioma

Peidang Liu[1,2]
Haizhen Jin[1]
Zhirui Guo[3]
Jun Ma[4]
Jing Zhao[1]
Dongdong Li[1]
Hao Wu[2]
Ning Gu[2]

[1]School of Medicine, [2]State Key Laboratory of Bioelectronics, Jiangsu Key Laboratory for Biomaterials and Devices, Southeast University, [3]The Second Affiliated Hospital of Nanjing Medical University, [4]Traditional Chinese Medicine Hospital of Jiangsu Province, Nanjing, People's Republic of China

Correspondence: Peidang Liu
School of Medicine, Southeast University, 87 Dingjiaqiao Road, Nanjing 210009, Jiangsu, People's Republic of China
Tel/fax +86 25 8327 2554
Email seulpd@163.com

Ning Gu
State Key Laboratory of Bioelectronics, Jiangsu Key Laboratory for Biomaterials and Devices, Southeast University, 4 Sipailou, Nanjing 210096, Jiangsu, People's Republic of China
Email guning@seu.edu.cn

Abstract: Radiotherapy performs an important function in the treatment of cancer, but resistance of tumor cells to radiation still remains a serious concern. More research on more effective radiosensitizers is urgently needed to overcome such resistance and thereby improve the treatment outcome. The goal of this study was to evaluate and compare the radiosensitizing efficacies of gold nanoparticles (AuNPs) and silver nanoparticles (AgNPs) on glioma at clinically relevant megavoltage energies. Both AuNPs and AgNPs potentiated the in vitro and in vivo antiglioma effects of radiation. AgNPs showed more powerful radiosensitizing ability than AuNPs at the same mass and molar concentrations, leading to a higher rate of apoptotic cell death. Furthermore, the combination of AgNPs with radiation significantly increased the levels of autophagy as compared with AuNPs plus radiation. These findings suggest the potential application of AgNPs as a highly effective nano-radiosensitizer for the treatment of glioma.

Keywords: gold nanoparticles, silver nanoparticles, radiosensitization, glioma, apoptosis, autophagy

Introduction

Malignant gliomas are the most common form of primary brain tumors, commonly producing progressive and profound disability and ultimately leading to death in most cases.[1] The current treatment regimen for this disease usually consists of surgical resection, radiotherapy, and, for some tumors, chemotherapy. Despite advances in the multimodality treatment in the past few decades, the prognosis of patients with high-grade gliomas, in particular glioblastoma multiformes, is still dismal. The median survival of patients with glioblastomas is only 7–15 months after diagnosis.[2] Radiation therapy provides a survival benefit, but resistance of glioma cells to radiation limits the therapeutic efficacy of this standard adjuvant treatment.[3] Therefore, innovative approaches are urgently needed to overcome such resistance and thereby enhance the treatment outcome.

Nano-sized materials, with size similar to most biological molecules, possess much potential for a wide variety of applications in the biomedical field. Recently, the addition of metal-based nanoparticles has been proposed as a novel strategy to improve the therapeutic index of radiation therapy.[4] Among these nanomaterials, gold nanoparticles (AuNPs) received a great deal of attention owing to their attractive properties, such as good biocompatibility, chemical stability, ease of surface modification, and high X-ray absorption coefficients.[5] Studies have implicated that the biological mechanisms of AuNPs radiosensitization may be involved in cell cycle

arrest and oxidative stress-mediated apoptosis, necrosis, or DNA damage.[6–8] The effectiveness of AuNPs as a potential radiation sensitizer has been determined in multiple cancer cell lines and radiation sources and through Monte Carlo calculations.[5] However, whether AuNPs can also sensitize glioma cells to radiation at clinically relevant megavoltage energies is still unclear.

Silver nanoparticles (AgNPs) are well known for their broad-spectrum antibacterial, antiviral, and anticancer effects.[9] More recently, AgNPs have been becoming another research hotspot in the field of radiation. Earlier studies by our group demonstrated the radiosensitivity effect of AgNPs on glioma both in vitro and in vivo.[10,11] Treating the malignant cells with AgNPs induced concentration- and size-dependent cytotoxicity at relatively harmless radiation doses.[10] Importantly, the in vivo study showed that the combination of AgNPs and radiotherapy resulted in a marked enhancement in mean survival time (MST), and an ~40% cure rate in glioma-bearing rats, which may be due to its potent antiproliferative activity.[11] Moreover, the enhanced radiation effects of silver nanomaterials were also observed in other different cancer cell lines, including hepatocellular carcinoma, gastric cancer, and breast cancer.[12–14] Overall, these results indicate that AgNPs can act as a promising radiosensitizer.

To promote the development of nano-radiosensitizers for clinical application, the efficacies of both AuNPs and AgNPs need to be established. The aim of this study was therefore to evaluate and compare the in vitro and in vivo radiosensitizing efficacies of AuNPs and AgNPs on glioma at megavoltage energies and to assess the possible underlying mechanisms of radiation dose enhancement effects of these two noble metal nanoparticles.

Materials and methods
Synthesis of AuNPs and AgNPs

AuNPs were synthesized by the classic citrate reduction method. Typically, 100 mL of an aqueous solution of 0.25 mM $HAuCl_4$ was heated to boiling for at least 3 minutes. Then, 3 mL of an aqueous solution of 1% trisodium citrate was added at one spot, and boiling was continued for 20 minutes during which the color of the solution turned from pale yellow to colorless, then light red, and finally ruby red. The citrate-capped AuNP solution was cooled naturally to room temperature for future use.

Synthesis of AgNPs was achieved by a seed-mediated approach as reported elsewhere.[15] Then, 4 nm AgNPs were used as seeds. For their synthesis, a mixture of 20 mL 1% citrate solution and 75 mL water was heated to 70°C. Under vigorous stirring, 1.7 mL of 1% $AgNO_3$ solution

was introduced to the mixture, followed by quickly adding 2 mL of 0.1% freshly prepared $NaBH_4$ solution. The solution was then diluted to 100 mL with water. In the next step, stepwise growth process was employed. Then, 2 mL of 1% citrate solution mixed with 75 mL water was heated to boiling, stirred vigorously, and followed by the addition of 10 mL seed solution and 0.35 mL 1% $AgNO_3$ solution, in order. The stirring continued for 30 minutes while keeping reflux. Finally, the citrate-capped AgNPs solution was cooled naturally to room temperature.

Characterization of AuNPs and AgNPs

The synthesized nanoparticles were primarily characterized by ultraviolet (UV)–visible spectroscopy (Shimadzu UV-3600; Japan) followed by transmission electron microscopy (TEM, JEM-2000EX; JEOL, Tokyo, Japan). TEM specimens were prepared by placing a few drops of sample solution on carbon-coated copper grids and drying at room temperature. The mean sizes, standard deviations, and size distributions were calculated by measuring more than 200 particles in random fields of view, in addition to the images that show general morphologies of the nanoparticles. The hydrodynamic diameters and zeta potentials were measured by dynamic light scattering using a Zetasizer Nano ZS (Malvern Instruments, Malvern, UK). The final concentrations of gold and silver in aqueous solution were determined by inductively coupled plasma mass spectrometry using Optima 5300DV (PerkinElmer Inc., Waltham, MA, USA).

Cell cultures

U251 glioblastoma cells were purchased from the Type Culture Collection of the Chinese Academy of Sciences (Shanghai, People's Republic of China). Cell culture media and reagents were purchased from Thermo Fisher Scientific (Waltham, MA, USA). All the cells used in this research were grown continuously as a monolayer in Dulbecco's Modified Eagle's Medium supplemented with 10% fetal bovine serum, penicillin, and streptomycin at 37°C in an atmosphere of 5% CO_2.

Distribution of nanoparticles in cells

U251 cells were grown in six-well plates and treated with 10 µg/mL of AuNPs or AgNPs for 24 hours. After harvesting, cell pellet was fixed in phosphate-buffered saline (PBS) solution containing 2% glutaraldehyde for 1 hour. After postfixing in 1% osmium tetroxide at room temperature for 60 minutes, cells were dehydrated with a graded series of ethanol and embedded in epoxy resin. Areas containing cells were block mounted and cut with an ultramicrotome and stained with

uranyl acetate followed by lead citrate. Finally, the ultrathin sections were examined under TEM (JEM-2000EX).

Cell viability assay

Cell viability was assessed by a Cell Counting Kit-8 (CCK-8; KeyGEN, People's Republic of China) assay according to the manufacturer's instruction. Human glioma U251 cells were seeded into 96-well plates and incubated for 24 hours prior to the treatment with the indicated concentrations of AuNPs, AgNPs, or vehicle. After treatment, CCK-8 reagent was added to each well and the cells were incubated for an additional 4 hours. The absorbance value at 490 nm was detected using a microplate reader (SpectraMax M5; Molecular Devices LLC, Sunnyvale, CA, USA). The cells treated with AuNPs or AgNPs were the experimental measurements (Read A); at the same time, media plus nanoparticles were used as the condition controls (Read B). The cells untreated with nanoparticles were set as the negative control (Read C). The effect of nanoparticles on cells was expressed as the percentage of cell viability calculated by the following formula:

$$\text{Cell viability}(\%) = \frac{(A-B)}{(C-B)} \times 100\% \qquad (1)$$

IC$_{50}$ was calculated using GraphPadPrism software (Version 6.0; GraphPad Software, Inc., La Jolla, CA, USA).

Radiation treatment

The cells were trypsinized and dispensed with different densities in different culture plates depending on the experimental requirements. Six different mass concentrations (0 µg/mL, 5 µg/mL, 10 µg/mL, 20 µg/mL, 40 µg/mL, or 80 µg/mL) or seven molar concentrations (0 µM, 25 µM, 50 µM, 50.76 µM, 100 µM, 200 µM, or 400 µM) of AuNPs or AgNPs were added into the medium following adherence of the cells. After 24 hours, cells were washed twice with PBS to remove the excess nanoparticles, and then irradiated by beams of 6 MV X-rays generated from a linear accelerator (Primus-M; Siemens, Germany) at a dose rate of 200 cGy/min. At the same time, control cells were removed from the incubator without radiation exposure.

Assay for clonogenic survival

The effectiveness of the combination of AuNPs or AgNPs with ionizing radiation was assessed by colony formation assays. U251 cells were cultured in six-well plates at 37°C and 5% CO$_2$ in a humidified incubator. After 70% population, cells were incubated for another 24 hours with or without the nanoparticles at the same mass (10 µg/mL for AuNPs and AgNPs [same mass concentration of AgNPs, mas-AgNPs]) and molar concentrations (50.76 µM for AuNPs [10 µg/mL] and AgNPs [same molar concentration of AgNPs, mol-AgNPs: 5.48 µg/mL]). Then, cells were washed twice with PBS before X-ray radiation. After radiation, cells were trypsinized and diluted, ~200 cells in control, radiation alone, and cotreated groups. Cells were cultured in 35 mm Petri dishes for 14 days, after which time they were fixed and stained with crystal violet. Each point on the survival curve represents the mean surviving fraction from at least three replicates. The sensitization enhancement ratio was calculated by determining the ratio of the D_0 of the control group vs experimental group.

Apoptosis assay

Apoptosis detection was performed using the Annexin V-FITC/propidium iodide (PI) Apoptosis Detection Kit (KeyGEN) according to the manufacturer's protocol. Briefly, following the treatment as described earlier, U251 cells were collected, washed in PBS twice, and then stained with Annexin-V and PI for 15 minutes at room temperature avoiding light. The cells were immediately analyzed by flow cytometry (FACSCalibur, BD, USA). Approximately 1×10^5 cells were analyzed in each of the samples. The assays were independently performed by two of the authors in a blinded manner.

Evaluation of acidic vesicular organelles

Formation of acidic vesicular organelles (AVOs), a characteristic of autophagy, was monitored by acridine orange (AO) and monodansylcadaverine (MDC) staining. U251 cells in 35 mm coverslip-bottomed dishes were treated with 5 µg/mL AO (Sigma-Aldrich Co., St Louis, MO, USA) and 0.05 mM MDC (Sigma-Aldrich Co.) in serum-free medium for 15 minutes and 30 minutes at 37°C, respectively. Subsequently, the cells were washed three times with PBS and immediately visualized with a BX53 Fluorescence Microscopy (Olympus Corporation, Tokyo, Japan). A total of 200 cells were counted for each variable.

Immunofluorescence staining for light chain 3

U251 cells were cultured on glass coverslips and treated as described earlier. Cells were fixed in 4% paraformaldehyde, permeabilized with 0.2% Triton X-100, and blocked with 0.2% bovine serum albumin for 30 minutes. Fixed cells were incubated with primary antibodies specific for microtubule-associated protein light chain 3 (LC3, 1:200; Novus, USA)

at 4°C overnight. After washing, cells were labeled with FITC-conjugated anti-rabbit IgG (1:100) for 1.5 hours at room temperature in the dark. After washing again, the cells were counterstained with 4′,6-diamidino-2-phenylindole and visualized with a fluorescence microscope (Olympus Corporation).

In vivo anti-glioma efficacy

The in vivo anti-glioma efficacy of AuNPs and AgNPs in combination with radiotherapy was evaluated by an orthotopic mouse brain tumor model. The intracranial U251 glioma model was established by inoculation of 5×10^5 cells (in 5 μL PBS) into the right striatum (2 mm lateral, 0.5 mm anterior to the bregma, and 3 mm of depth) of female BALB/c nude mice by using a small animal stereotactic frame (RWD Life Science, Shenzhen, People's Republic of China). The glioma-bearing mice were randomly divided into eight groups (n=7): untreated control, AuNPs, mas-AgNPs, mol-AgNPs, radiated control, AuNPs plus radiation, mas-AgNPs plus radiation, and mol-AgNPs plus radiation. Then, 4 μL of deionized water, AuNPs (10 μg), or AgNPs (10 μg or 5.48 μg) were intratumorally administered using stereotactic technique 12 days post-inoculation. Approximately 24 hours after the injection of nanomaterials, mice were anesthetized by a peritoneal injection with 5 μL/g of 7.5% chloral hydrate and immobilized with a fixed apparatus, and the tumor ipsilateral half brain was radiated by a vertical beam of 6 MV X-rays. The delivered dose was 8 Gy per mouse. After treatment with nanoparticles by injection, the animals were examined daily for any changes in clinical appearance and weighed thrice a week. The survival time was recorded and used in the survival analysis. The use of animals in this study was approved by the Institutional Animal Care and Use Committee of the Southeast University.

Statistical analysis

All data were expressed as mean ± standard deviation. Statistical significance was determined using one-way ANOVA followed by a Tukey–Kramer post hoc test. The survival analysis was performed using the Kaplan–Meier survival curve and the log-rank test. A value of $P < 0.05$ was considered significantly different.

Results and discussion
Synthesis and characterization of AuNPs and AgNPs

It is well known that particle size is an important factor in the biological environment. AuNPs and AgNPs have a size-dependent cytotoxicity, the smaller the size the more toxic they may be,[16,17] since smaller nanomaterials have a greater surface area to volume ratio and hence a much higher reactivity. On the other hand, some studies have suggested that AuNPs and AgNPs ranging in size from 10 nm to 20 nm have better radiosensitizing effects.[10,18] Taking these considerations into account, 15 nm AuNPs and AgNPs with the same coating were synthesized and used in the current study.

The size distribution and optical absorption of the citrate-stabilized nanoparticles are characterized by TEM and spectrophotometry as shown in Figure 1. The AuNPs and AgNPs synthesized in colloidal solution were predominantly spherical in morphology with good monodispersity and average sizes of 15.36±2.48 nm and 15.26±3.92 nm, respectively (Figure 1A–D). UV–visible spectroscopy displayed absorption peaks at 515 nm for AuNPs and 392 nm for AgNPs (Figure 1E and F), which were in accordance with the characteristic surface plasmon resonance absorption bands of the corresponding nanoparticles. The citrate-coated AuNPs and AgNPs were also analyzed by dynamic light scattering that showed hydrodynamic diameters of 20.64±0.03 nm and 26.75±0.05 nm, polydispersity index of 0.29±0.05 and 0.25±0.04, and zeta potentials of −35.30±0.70 mV and −35.23±1.35 mV, respectively.

Intracellular localization of AuNPs and AgNPs

Intracellular localization of nanomaterials plays an important and direct role in executing their biomedical functions or in toxicity.[19] The localization of AuNPs and AgNPs inside U251 glioma cells was thus investigated by using TEM. Untreated cells that were free of the nanoparticles were used as a control (Figure 2A). As shown in Figure 2B and C, U251 cells that were treated with 10 μg/mL AuNPs or AgNPs evidently internalized the nanoparticles, which were aggregated and mainly localized in the endosomes, suggesting that the AuNPs and AgNPs enter the cells most likely via endocytosis. The results of AuNPs and AgNPs are consistent with the findings of earlier studies.[20,21]

Effects of AuNPs and AgNPs on cell viability

Due to their diversified physicochemical properties, different nanoparticles may exert distinct biological effects and cytotoxicity.[22] To evaluate the differential growth inhibitory effects of AuNPs and AgNPs on U251 cells, the CCK-8 cell viability assay was performed. The results showed that both AuNPs and AgNPs caused a dose-dependent reduction of cell viability in
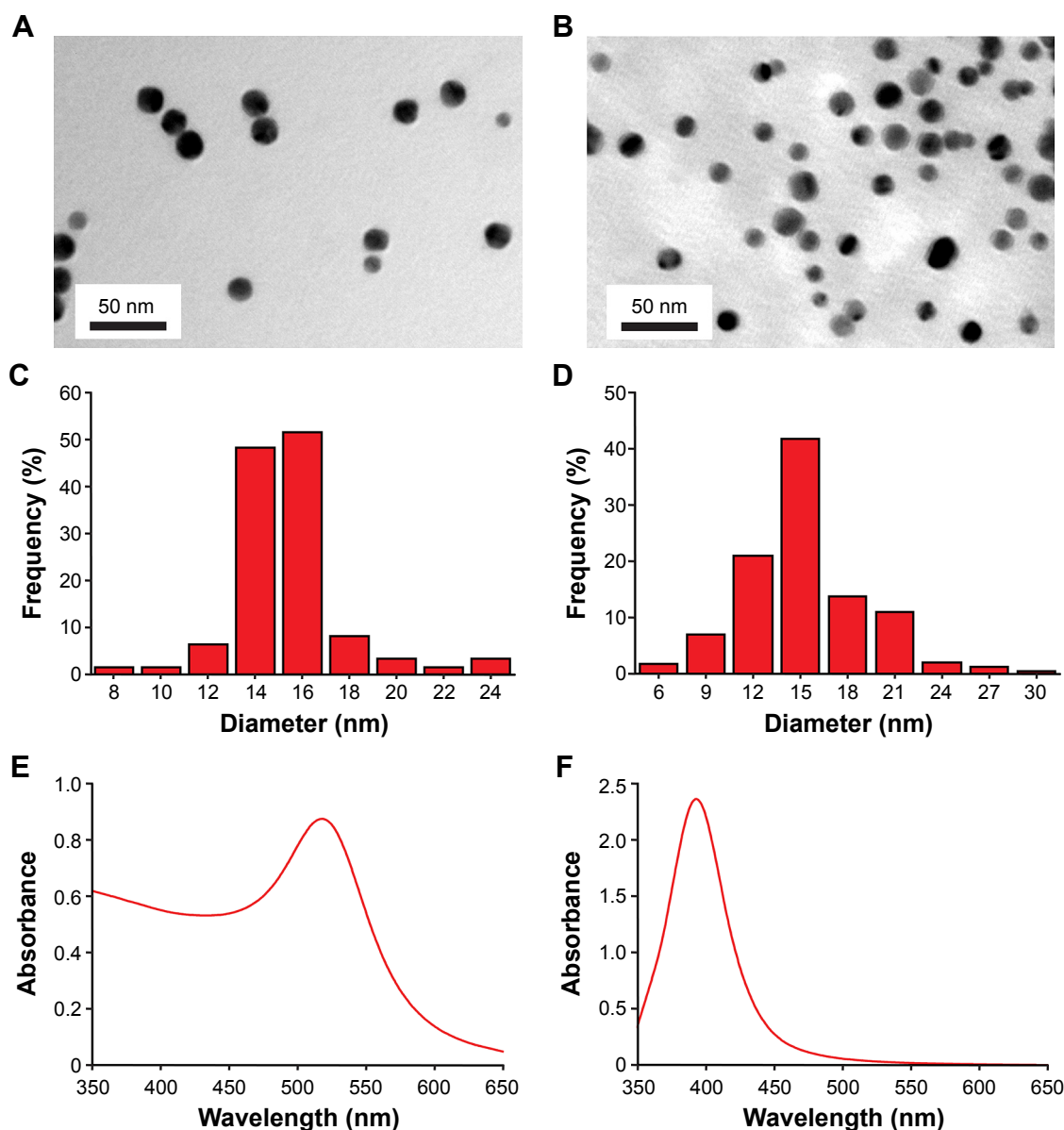
Figure 1 TEM characterization and UV–visible absorption spectra of AuNPs and AgNPs.
Notes: Particles were spotted onto carbon-coated Cu grids and dried under air prior to TEM imaging. The particle size distributions were determined by measuring the nanoparticles from micrographs using ImageJ with n>200 for each sample. TEM (**A**), size distribution (**C**) and UV–visible absorption spectrum (**E**) of AuNPs. TEM (**B**), size distribution (**D**) and UV–visible absorption spectrum (**F**) of AgNPs.
Abbreviations: AgNPs, silver nanoparticles; AuNPs, gold nanoparticles; TEM, transmission electron microscopy; UV, ultraviolet.

U251 cells (Figure 3), but had little effect on a noncancerous cell line (Figure S1). There was no significant difference between AuNPs and AgNPs at the same molar concentrations ($P>0.05$); however, at the same mass concentrations, AgNPs significantly increased growth inhibition of the glioma cells compared with AuNPs at concentrations exceeding 10 μg/mL ($P<0.05$ or $P<0.001$). The IC_{50} values obtained for AuNPs and AgNPs were 116.3 μg/mL and 75.9 μg/mL, respectively.

It has been found that AgNPs could elicit toxic and anti-proliferative effects against cancer cells and could therefore be utilized as a potent therapeutic agent for cancers.[23,24]

Interestingly, in recent years, AuNPs have also been reported to show anticancer and antimetastatic properties without any functionalization, indicating that AuNPs may serve as self-therapeutic nanomaterial particles.[25,26] In the current study, we demonstrated that AgNPs could significantly exhibit stronger inhibitory effect on U251 glioma cells than AuNPs. Since the deposition of metal nanoparticles inside the nucleus could affect cell division and damage DNA through direct interaction,[24,27] currently, nuclear-targeted modification of AuNPs and AgNPs has been explored as a new route to improve their cancer treatment outcome.[28,29]
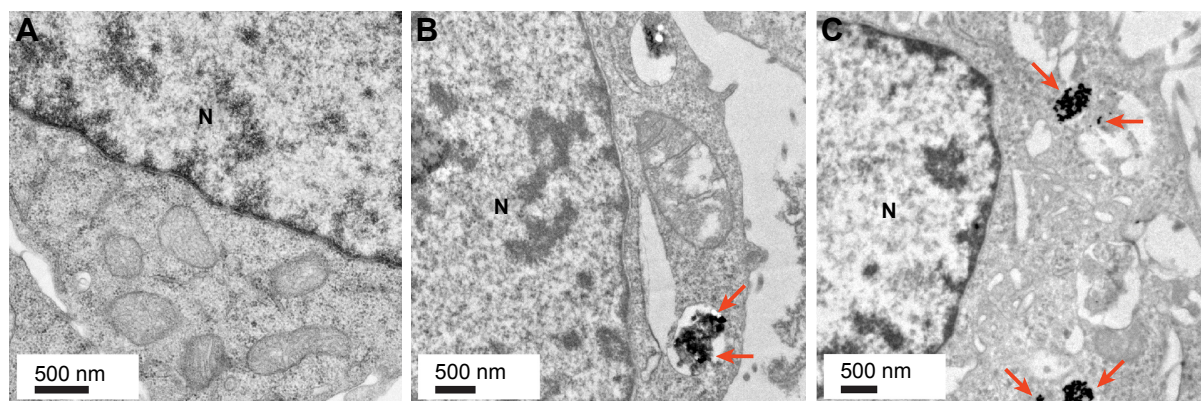
Figure 2 Localization of AuNPs and AgNPs in U251 cells.
Notes: (**A**) The representative TEM image of control cells. The representative images of U251 cells treated with 10 μg/mL AuNPs and AgNPs for 24 hours are shown in (**B**) and (**C**), respectively. Nanoparticle aggregates visible mainly in endosomes as black and electron-dense spots are indicated by arrows.
Abbreviations: AgNPs, silver nanoparticles; AuNPs, gold nanoparticles; N, nucleus; TEM, transmission electron microscopy.

Many factors including surface coatings may influence nanoparticle toxicity.[30] In this study, we investigated the effect of the citrate coating. Citrate-coated and naked AgNPs exhibited similar cytotoxicity (Figure S2). This data indicated that the citrate coating did not show a significant impact on the toxicity of nanoparticles.

Radiosensitizing efficacies of AuNPs and AgNPs

To determine and compare the radiation-sensitizing efficacies of AuNPs and AgNPs on glioma, we performed the in vitro and in vivo experiments. First, colony formation assay, the gold standard for detecting radiosensitivity,[31] was carried out to evaluate the long-term proliferation inhibition of U251 cells. The radiation dose-dependent radiosensitizing data of AuNPs and AgNPs are shown in Figure 4. As shown in the figure, the surviving fraction decreased sharply with increasing doses of 6 MV X-rays, and there was a significant separation between the curves, suggesting that both AuNPs and AgNPs can enhance the effect of radiation on glioma cells. It is worthy to note that mas-AgNPs showed the highest radiosensitizing activity, followed by mol-AgNPs and finally by AuNPs. The corresponding sensitization enhancement ratios are 1.64, 1.44, and 1.23, respectively. This difference was again demonstrated by the short-term (CCK-8) assay (Figure 3). In addition, the radiosensitization appeared to
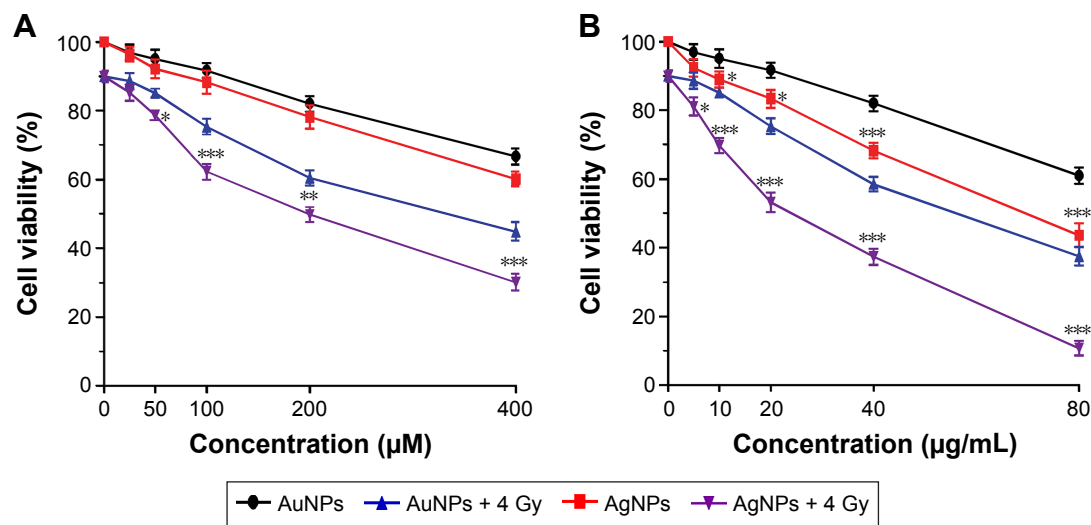

Figure 3 Effects of AuNPs and AgNPs on U251 cell viability with or without radiation.
Notes: Cells were incubated for 24 hours with varying concentrations of AuNPs or AgNPs. At 24 hours after radiation treatment, cell viability was determined using a CCK-8 assay. The cell viabilities at the same molar and mass concentrations are shown in (**A**) and (**B**), respectively. Data are a summary of three independent experiments and expressed as mean ± SD. *$P<0.05$, **$P<0.01$, ***$P<0.001$ compared with the corresponding AuNPs-treated group.
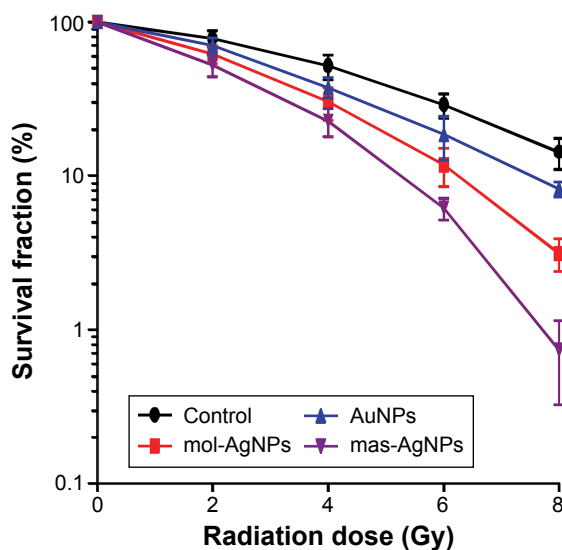**Abbreviations:** AgNPs, silver nanoparticles; AuNPs, gold nanoparticles; CCK-8, Cell Counting Kit-8; SD, standard deviation.

Figure 4 Effects of AuNPs and AgNPs in combination with radiation on colony formation of U251 cells.
Note: Data are represented as mean ± SD from three different samples.
Abbreviations: AgNPs, silver nanoparticles; AuNPs, gold nanoparticles; mas-AgNPs, same mass concentration of AgNPs; mol-AgNPs, same molar concentration of AgNPs; SD, standard deviation.
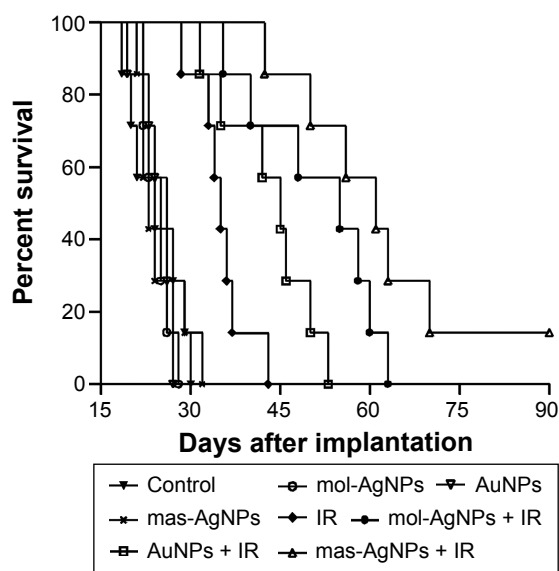

Figure 5 Kaplan–Meier survival curves for U251 glioma-bearing mice following intratumoral administration of AuNPs or AgNPs with or without radiation.
Notes: Deionized water (4 μL), AuNPs (10 μg), or AgNPs (10 μg or 5.48 μg) were intratumorally administered 12 days post-inoculation. At day 13, mice were irradiated with a single dose of 6 MV X-rays (8 Gy/mouse, n=7 mice/group).
Abbreviations: AgNPs, silver nanoparticles; AuNPs, gold nanoparticles; IR, ionizing radiation; mas-AgNPs, same mass concentration of AgNPs; mol-AgNPs, same molar concentration of AgNPs.

be tumor cell specific, because this effect was not apparent in noncancerous cells (Figure S3).

To further determine whether the combination of AgNPs and radiotherapy resulted in better in vivo antitumor effects in terms of survival than AuNPs plus radiation, the radiotherapy was performed following intratumoral administration of AgNPs or AuNPs, and the survival time of the tumor-bearing mice was recorded and analyzed. Kaplan–Meier survival plots are shown in Figure 5. The radiated controls had a modest increase in MST to 35.1 days compared with an MST of 24.1 days for the untreated mice. Furthermore, the overall survival time of the three combination therapy groups was significantly longer than that of radiation alone group. More importantly, animals that received mas-AgNPs, mol-AgNPs, and AuNPs combined with radiotherapy had MSTs of 61.7 days, 51.3 days, and 43.1 days, respectively, which were statistically significant between AgNPs and AuNPs associated with radiotherapy groups ($P<0.05$ or $P<0.01$). The order of sensitizing ability was mas-AgNPs > mol-AgNPs > AuNPs. Clearly, these in vivo antitumor data in an orthotopic xenograft model system confirmed our in vitro findings.

Energy of irradiating X-ray beam affects X-ray absorption by nanoparticles and plays an important role in dose enhancements.[32] It is widely accepted that the use of low-energy kilovoltage beams could maximize tumor dose enhancement;[33,34] however, their inherent shallow penetration

and significant dose heterogeneity inside the target tumor hinder the translation of this technology to the clinic.[35] Compared with kilovoltage, the clinically relevant megavoltage X-ray energies have relatively limited application in the field of nanoparticle-based radiotherapy. In this study, we demonstrated the efficacies of AuNPs and AgNPs in conjunction with a single moderate dose of 6 MV radiation with the latter being the stronger. The hypothesized mechanism is that these nanoparticles could produce additional short-range secondary electrons once activated by megavoltage X-ray beams. These low-energy electrons then generate large amounts of free radicals, which amplify and prolong the deleterious effects of radiotherapy.[36,37]

Proapoptotic effects of AuNPs and AgNPs combined with radiotherapy

Increasing research has evidenced that apoptosis contributes significantly to radiation therapy-induced tumor cell death and to the radiosensitivity of tumor cells.[38,39] In the current study, the apoptotic response of U251 cells to AuNPs or AgNPs with or without radiation was evaluated by Annexin V-FITC/PI assay. As shown in Figure 6A and B, only mas-AgNPs alone treatment led to a marked enhancement in apoptotic cell death compared with the untreated control ($P<0.001$). There was a slight but significant difference
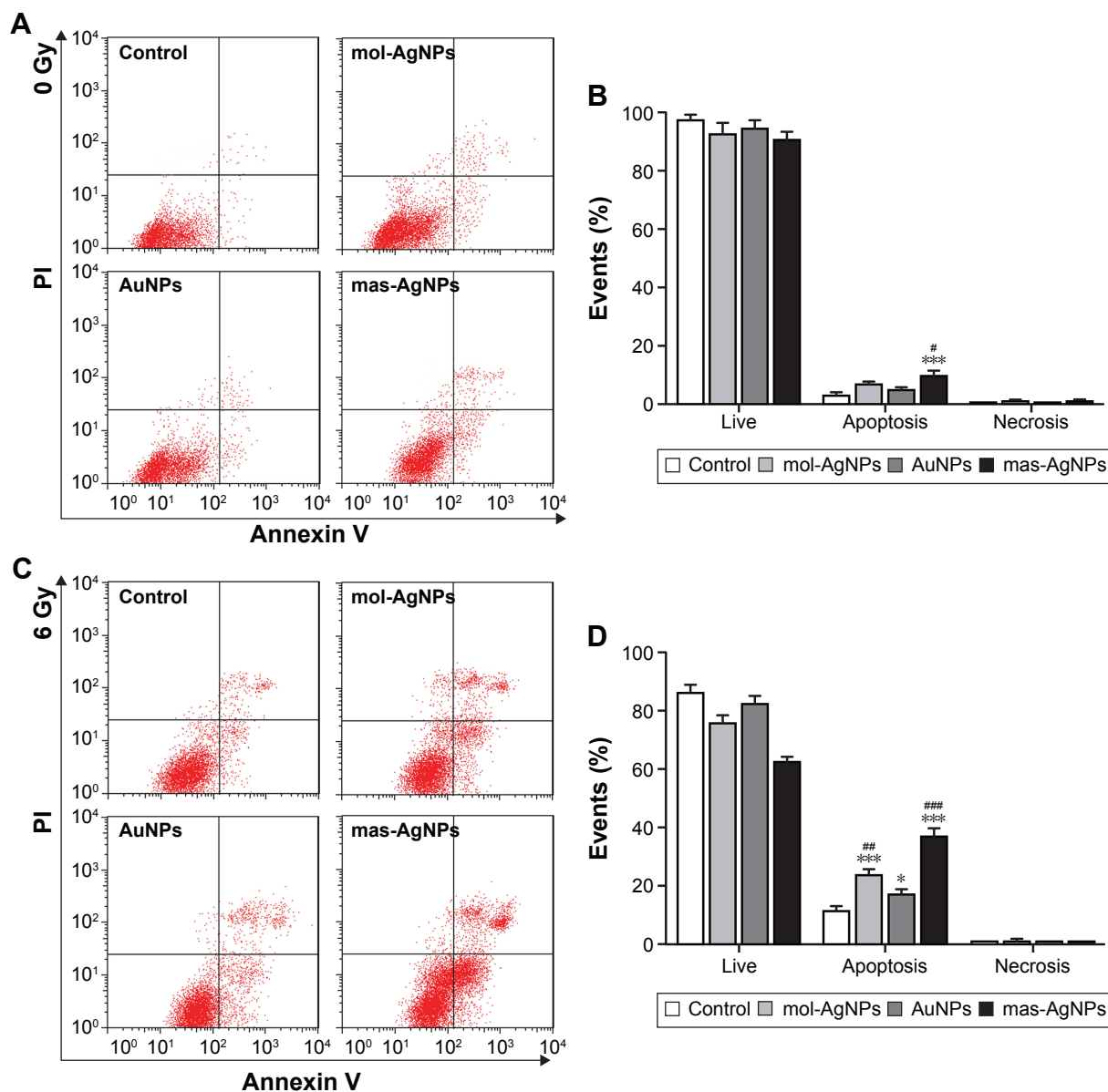
Figure 6 Apoptosis of U251 cells induced by AuNPs and AgNPs with or without radiation.
Notes: The apoptosis rates of U251 cells treated with 50.76 μM or 10 μg/mL AuNPs or AgNPs, followed by 6 Gy radiation, or without, were determined by flow cytometry using Annexin V-FITC and PI as probes. Representative images and summary of distributions of cell status without and with radiation are shown in (**A**), (**B**) and (**C**), (**D**), respectively. *$P < 0.05$, ***$P < 0.001$ compared with the control group. #$P < 0.05$, ##$P < 0.01$, ###$P < 0.001$ compared with the corresponding AuNPs-treated group.
Abbreviations: AgNPs, silver nanoparticles; AuNPs, gold nanoparticles; mas-AgNPs, same mass concentration of AgNPs; mol-AgNPs, same molar concentration of AgNPs; PI, propidium iodide.

between mas-AgNPs- and AuNPs-treated groups ($P < 0.05$). The addition of AuNPs or AgNPs drastically increased the radiation-induced apoptotic index as compared to the radiation control (Figure 6C and D; $P < 0.05$ or $P < 0.001$). As expected, the levels of apoptosis were significantly higher in the AgNPs and radiation combination groups than that in the AuNPs plus radiation group ($P < 0.01$ or $P < 0.001$). However, there was no significant change in the percentage of necrotic cells between the three nanoradiotherapy groups. These results indicated that the radiosensitizing effects of

AuNPs and AgNPs were associated with apoptosis but not necrosis, and that the better radiosensitizing performance of AgNPs may result from higher apoptosis induction.

Promotion of autophagy by AuNPs or AgNPs in combination with radiation

Autophagy has been shown to play an important role in cancer cell survival and death.[40,41] To determine whether the combination of AuNPs or AgNPs with ionizing radiation increased the levels of autophagy, AO, MDC, and LC3 puncta were

monitored and quantified. Figure 7A–D indicates that, based on AO and MDC staining, no or little autophagy was detectable in untreated control cells, while AuNPs or AgNPs alone increased the formation of AVOs, suggesting the upregulation of autophagy. The combined treatment with these nanoparticles and radiation further enhanced the development of AVOs. Quantitative evaluation showed that AgNPs in conjunction with radiation significantly increased the number of AVOs per cell as compared with AuNPs plus radiation (Figure 7B and D;

$P<0.01$ or $P<0.001$). The promotion of autophagy by AuNPs and AgNPs with or without radiation was also confirmed by LC3 redistribution. Upon autophagy activation, lipidated LC3, a specific marker for autophagosomes, exhibits a puncta staining pattern in the cytoplasm.[42] The immunohistochemistry results showed that, consistent with AO and MDC staining, there was a significant difference in the number of LC3 punctate dots per cell between AuNPs + radiation and AgNPs + radiation (Figure 7E and F; $P<0.001$).
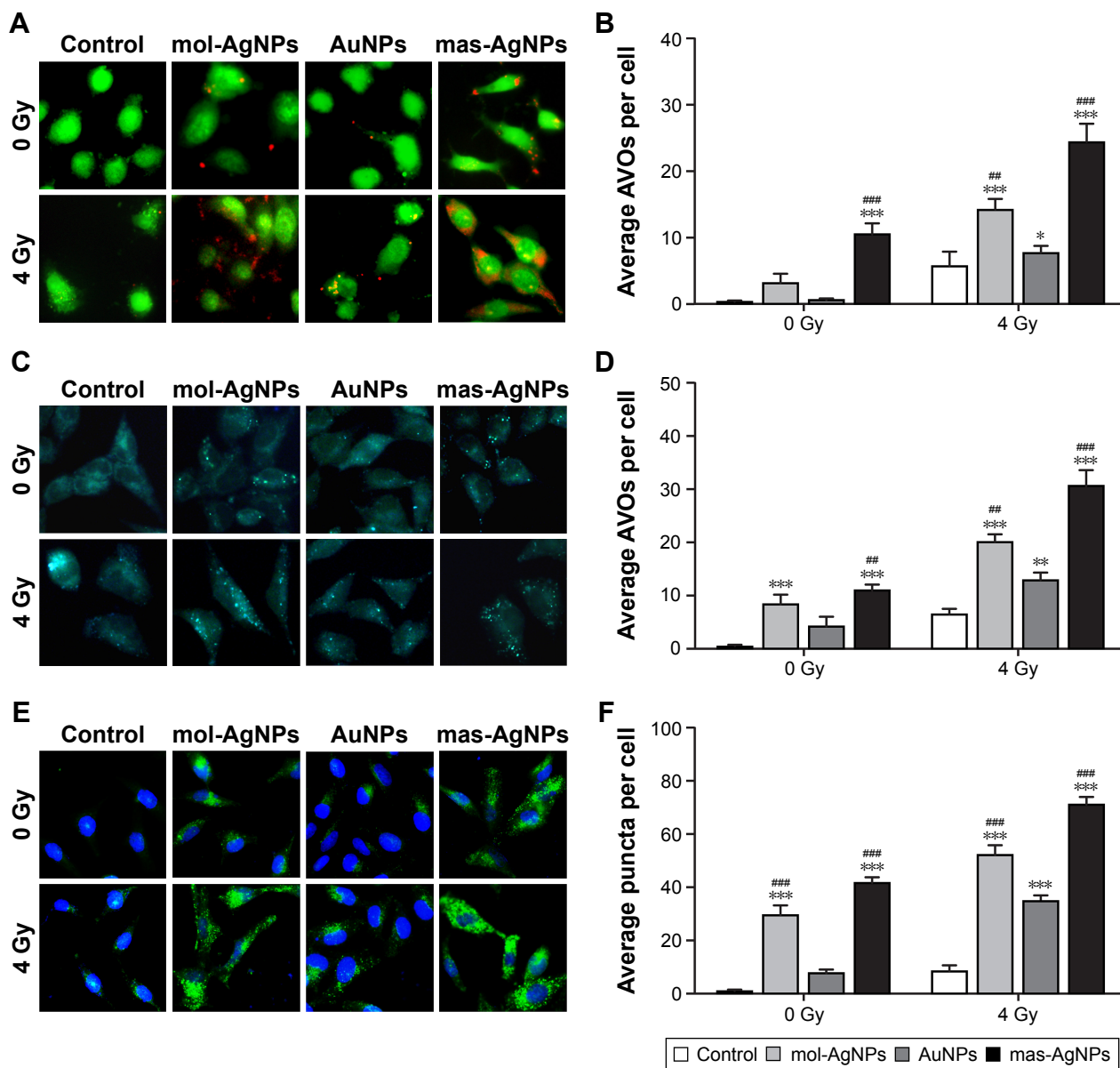

Figure 7 Promotion of autophagy by AuNPs and AgNPs with or without radiation in U251 cells.
Notes: U251 cells were incubated for 24 hours with 50.76 μM or 10 μg/mL AuNPs or AgNPs. At 24 hours after 4 Gy radiation treatment, cells were stained for AO, MDC or LC3, and visualized with fluorescence microscopy. (**A**) Representative images and (**B**) average number of AVOs per cell of AO staining. (**C**) Representative images and (**D**) average number of AVOs per cell of MDC staining. (**E**) Representative images and (**F**) average number of puncta per cell of LC3 immunofluorescence staining. *$P<0.05$, **$P<0.01$, ***$P<0.001$ compared with the corresponding control group. ##$P<0.01$, ###$P<0.001$ compared with the corresponding AuNPs-treated group.
Abbreviations: AgNPs, silver nanoparticles; AO, acridine orange; AuNPs, gold nanoparticles; AVOs, acidic vesicular organelles; LC3, microtubule-associated protein light chain 3; mas-AgNPs, same mass concentration of AgNPs; MDC, monodansylcadaverine; mol-AgNPs, same molar concentration of AgNPs.

As a critical degradation process of cytoplasmic components, autophagy is involved in maintaining cellular homeostasis and functions.[43] Up to now, a variety of nanosized materials, such as graphene, quantum dots, iron oxide, and rare earth nanocrystals, have been proved to elicit autophagic responses in multiple cancer cell lines.[44–47] In the current study, we found that AuNPs and AgNPs could act as inducers of autophagy, which are in line with earlier reports.[48,49] The mechanism of AuNPs leading to autophagosome accumulation is due to the blockade of autophagy flux, while that of AgNPs the induction of autophagy.[49,50] Moreover, we further demonstrated that their combination with radiation induced greater levels of autophagy in glioma cells. Although autophagy is originally defined as type II programmed cell death, researchers have disclosed that autophagy also plays a dual role in cancer development, progression, and treatment.[51] Contrary to the role of autophagy triggered by most nanomaterials, our recently reported studies have revealed that autophagy initiated by AgNPs or/and radiation mediates cytoprotective effect, which is believed to serve as a pro-survival process of cells facing AgNPs and their associated radiation.[49,52] Given that both AuNPs and AgNPs belong to the noble metal nanoparticles, and the roles of their enhanced autophagy are the same,[49,53] this could indicate that autophagy activated by AuNPs plus radiation may be similar in function to that by AgNPs plus radiation. Since protective autophagy antagonizes apoptotic cell death induced by cancer chemotherapy and radiation therapy,[54,55] pharmacological inhibition of this type of autophagy should enhance the anticancer activity of AuNPs alone, AgNPs alone, or their combination with radiation, in particular that of AgNPs-based treatment.

Conclusion

The purpose of the current study was to evaluate and compare the radiosensitizing efficacies of AuNPs and AgNPs, the two most focused nano-radiosensitizers, on glioma at megavoltage energies. The colony formation, survival time of glioma-bearing mice, cell apoptosis, and autophagy were investigated at the same mass and molar concentrations. It was found that the combination of AgNPs and radiotherapy showed significantly enhanced antiglioma effects in vitro and in vivo, when compared with AuNPs plus radiation, which may be due to its higher proapoptotic activity. In addition, the level of autophagy was also more strongly upregulated following the treatment of AgNPs with radiation, suggesting that modulation of the autophagy response may improve their therapeutic outcome. These findings will provide an important basis for selecting and applying the highly effective nano-radiosensitizer for the treatment of glioma. The differential radiosensitizing efficacies of AgNPs and AuNPs at other concentrations or with larger or smaller sizes need further investigation.

Disclosure

The authors report no conflicts of interest in this work.

References

1. Romanelli P, Conti A, Pontoriero A, et al. Role of stereotactic radiosurgery and fractionated stereotactic radiotherapy for the treatment of recurrent glioblastoma multiforme. *Neurosurg Focus*. 2009;27(6):E8.
2. Frosina G. Limited advances in therapy of glioblastoma trigger reconsideration of research policy. *Crit Rev Oncol Hematol*. 2015;96(2): 257–261.
3. Noda SE, El-Jawahri A, Patel D, Lautenschlaeger T, Siedow M, Chakravarti A. Molecular advances of brain tumors in radiation oncology. *Semin Radiat Oncol*. 2009;19(3):171–178.
4. Babaei M, Ganjalikhani M. The potential effectiveness of nanoparticles as radio sensitizers for radiotherapy. *Bioimpacts*. 2014;4(1):15–20.
5. Su XY, Liu PD, Wu H, Gu N. Enhancement of radiosensitization by metal-based nanoparticles in cancer radiation therapy. *Cancer Biol Med*. 2014;11(2):86–91.
6. Wang C, Jiang Y, Li X, Hu L. Thioglucose-bound gold nanoparticles increase the radiosensitivity of a triple-negative breast cancer cell line (MDA-MB-231). *Breast Cancer*. 2015;22(4):413–420.
7. Taggart LE, McMahon SJ, Currell FJ, Prise KM, Butterworth KT. The role of mitochondrial function in gold nanoparticle mediated radiosensitisation. *Cancer Nanotechnol*. 2014;5(1):5.
8. Zhang P, Qiao Y, Xia J, Guan J, Ma L, Su M. Enhanced radiation therapy with multilayer microdisks containing radiosensitizing gold nanoparticles. *ACS Appl Mater Interfaces*. 2015;7(8):4518–4524.
9. Rai M, Kon K, Ingle A, Duran N, Galdiero S, Galdiero M. Broadspectrum bioactivities of silver nanoparticles: the emerging trends and future prospects. *Appl Microbiol Biotechnol*. 2014;98(5):1951–1961.
10. Xu R, Ma J, Sun X, et al. Ag nanoparticles sensitize IR-induced killing of cancer cells. *Cell Res*. 2009;19(8):1031–1034.
11. Liu P, Huang Z, Chen Z, et al. Silver nanoparticles: a novel radiation sensitizer for glioma? *Nanoscale*. 2013;5(23):11829–11836.
12. Zheng Q, Yang H, Wei J, Tong JL, Shu YQ. The role and mechanisms of nanoparticles to enhance radiosensitivity in hepatocellular cell. *Biomed Pharmacother*. 2013;67(7):569–575.
13. Huang P, Yang DP, Zhang C, et al. Protein-directed one-pot synthesis of Ag microspheres with good biocompatibility and enhancement of radiation effects on gastric cancer cells. *Nanoscale*. 2011;3(9):3623–3626.
14. Swanner J, Mims J, Carroll DL, et al. Differential cytotoxic and radiosensitizing effects of silver nanoparticles on triple-negative breast cancer and non-triple-negative breast cells. *Int J Nanomedicine*. 2015;10: 3937–3953.

15. Wan Y, Guo Z, Jiang X, et al. Quasi-spherical silver nanoparticles: aqueous synthesis and size control by the seed-mediated Lee-Meisel method. *J Colloid Interface Sci*. 2013;394:263–268.

16. Pan Y, Neuss S, Leifert A, et al. Size-dependent cytotoxicity of gold nanoparticles. *Small*. 2007;3(11):1941–1949.

17. Liu W, Wu Y, Wang C, et al. Impact of silver nanoparticles on human cells: effect of particle size. *Nanotoxicology*. 2010;4(3):319–330.

18. Zhang XD, Wu D, Shen X, et al. Size-dependent radiosensitization of PEG-coated gold nanoparticles for cancer radiation therapy. *Biomaterials*. 2012;33(27):6408–6419.

19. Zhao F, Zhao Y, Liu Y, Chang X, Chen C, Zhao Y. Cellular uptake, intracellular trafficking, and cytotoxicity of nanomaterials. *Small*. 2011;7(10):1322–1337.

20. Huang K, Ma H, Liu J, et al. Size-dependent localization and penetration of ultrasmall gold nanoparticles in cancer cells, multicellular spheroids, and tumors in vivo. *ACS Nano*. 2012;6(5):4483–4493.

21. Zhang XF, Choi YJ, Han JW, et al. Differential nanoreprotoxicity of silver nanoparticles in male somatic cells and spermatogonial stem cells. *Int J Nanomedicine*. 2015;10:1335–1357.

22. Gatoo MA, Naseem S, Arfat MY, Dar AM, Qasim K, Zubair S. Physicochemical properties of nanomaterials: implication in associated toxic manifestations. *Biomed Res Int*. 2014;2014:498420.

23. Sriram MI, Kanth SB, Kalishwaralal K, Gurunathan S. Antitumor activity of silver nanoparticles in Dalton's lymphoma ascites tumor model. *Int J Nanomedicine*. 2010;5:753–762.

24. Asharani PV, Hande MP, Valiyaveettil S. Anti-proliferative activity of silver nanoparticles. *BMC Cell Biol*. 2009;10:65.

25. Arvizo RR, Saha S, Wang E, Robertson JD, Bhattacharya R, Mukherjee P. Inhibition of tumor growth and metastasis by a self-therapeutic nanoparticle. *Proc Natl Acad Sci U S A*. 2013;110(17):6700–6705.

26. Balasubramani G, Ramkumar R, Krishnaveni N, et al. Structural characterization, antioxidant and anticancer properties of gold nanoparticles synthesized from leaf extract (decoction) of *Antigonon leptopus* Hook. &Arn. *J Trace Elem Med Biol*. 2015;30:83–89.

27. Berbeco RI, Korideck H, Ngwa W, et al. DNA damage enhancement from gold nanoparticles for clinical MV photon beams. *Radiat Res*. 2012;178(6):604–608.

28. Kang B, Mackey MA, El-Sayed MA. Nuclear targeting of gold nanoparticles in cancer cells induces DNA damage, causing cytokinesis arrest and apoptosis. *J Am Chem Soc*. 2010;132(5):1517–1519.

29. Austin LA, Kang B, Yen CW, El-Sayed MA. Nuclear targeted silver nanospheres perturb the cancer cell cycle differently than those of nanogold. *Bioconjug Chem*. 2011;22(11):2324–2331.

30. Ai J, Biazar E, Jafarpour M, et al. Nanotoxicology and nanoparticle safety in biomedical designs. *Int J Nanomedicine*. 2011;6:1117–1127.

31. Nahas SA, Gatti RA. DNA double strand break repair defects, primary immunodeficiency disorders, and 'radiosensitivity'. *Curr Opin Allergy Clin Immunol*. 2009;9(6):510–516.

32. Hossain M, Su M. Nanoparticle location and material dependent dose enhancement in X-ray radiation therapy. *J Phys Chem C Nanomater Interfaces*. 2012;116(43):23047–23052.

33. Chithrani DB, Jelveh S, Jalali F, et al. Gold nanoparticles as radiation sensitizers in cancer therapy. *Radiat Res*. 2010;173(6):719–728.

34. Lin Y, Paganetti H, McMahon SJ, Schuemann J. Gold nanoparticle induced vasculature damage in radiotherapy: comparing protons, megavoltage photons, and kilovoltage photons. *Med Phys*. 2015;42(10):5890–5902.

35. Verhaegen F, Reniers B, Deblois F, Devic S, Seuntjens J, Hristov D. Dosimetric and microdosimetric study of contrast-enhanced radiotherapy with kilovolt X-rays. *Phys Med Biol*. 2005;50(15):3555–3569.

36. Liu J, Liang Y, Liu T, Li D, Yang X. Anti-EGFR-conjugated hollow gold nanospheres enhance radiocytotoxic targeting of cervical cancer at megavoltage radiation energies. *Nanoscale Res Lett*. 2015;10:218.

37. Meidanchi A, Akhavan O, Khoei S, Shokri AA, Hajikarimi Z, Khansari N. ZnFe2O4 nanoparticles as radiosensitizers in radiotherapy of human prostate cancer cells. *Mater Sci Eng C Mater Biol Appl*. 2015;46:394–399.

38. Rupnow BA, Knox SJ. The role of radiation-induced apoptosis as a determinant of tumor responses to radiation therapy. *Apoptosis*. 1999;4(2):115–143.

39. Verheij M, Bartelink H. Radiation-induced apoptosis. *Cell Tissue Res*. 2000;301(1):133–142.

40. Mizushima N. Autophagy: process and function. *Genes Dev*. 2007;21(22):2861–2873.

41. Eskelinen EL, Saftig P. Autophagy: a lysosomal degradation pathway with a central role in health and disease. *Biochim Biophys Acta*. 2009;1793(4):664–673.

42. Kabeya Y, Mizushima N, Ueno T, et al. LC3, a mammalian homologue of yeast Apg8p, is localized in autophagosome membranes after processing. *EMBO J*. 2000;19(21):5720–5728.

43. Li S, Wang L, Hu Y, Sheng R. Autophagy regulators as potential cancer therapeutic agents: a review. *Curr Top Med Chem*. 2015;15(8):720–744.

44. Markovic ZM, Ristic BZ, Arsikin KM, et al. Graphene quantum dots as autophagy-inducing photodynamic agents. *Biomaterials*. 2012;33(29):7084–7092.

45. Seleverstov O, Zabirnyk O, Zscharnack M, et al. Quantum dots for human mesenchymal stem cells labeling. A size-dependent autophagy activation. *Nano Lett*. 2006;6(12):2826–2832.

46. Khan MI, Mohammad A, Patil G, Naqvi SA, Chauhan LK, Ahmad I. Induction of ROS, mitochondrial damage and autophagy in lung epithelial cancer cells by iron oxide nanoparticles. *Biomaterials*. 2012;33(5):1477–1488.

47. Man N, Yu L, Yu SH, Wen LP. Rare earth oxide nanocrystals as a new class of autophagy inducers. *Autophagy*. 2010;6(2):310–311.

48. Li JJ, Hartono D, Ong CN, Bay BH, Yung LY. Autophagy and oxidative stress associated with gold nanoparticles. *Biomaterials*. 2010;31(23):5996–6003.

49. Lin J, Huang Z, Wu H, et al. Inhibition of autophagy enhances the anticancer activity of silver nanoparticles. *Autophagy*. 2014;10(11):2006–2020.

50. Ma X, Wu Y, Jin S, et al. Gold nanoparticles induce autophagosome accumulation through size-dependent nanoparticle uptake and lysosome impairment. *ACS Nano*. 2011;5(11):8629–8639.

51. Zhou S, Zhao L, Kuang M, et al. Autophagy in tumorigenesis and cancer therapy: Dr. Jekyll or Mr. Hyde? *Cancer Lett*. 2012;323(2):115–127.

52. Wu H, Lin J, Liu P, et al. Is the autophagy a friend or foe in the silver nanoparticles associated radiotherapy for glioma? *Biomaterials*. 2015;62:47–57.

53. Ding F, Li Y, Liu J, et al. Overendocytosis of gold nanoparticles increases autophagy and apoptosis in hypoxic human renal proximal tubular cells. *Int J Nanomedicine*. 2014;9:4317–4330.

54. Wang K, Liu R, Li J, et al. Quercetin induces protective autophagy in gastric cancer cells: involvement of Akt-mTOR- and hypoxia-induced factor 1alpha-mediated signaling. *Autophagy*. 2011;7(9):966–978.

55. Liang B, Kong D, Liu Y, et al. Autophagy inhibition plays the synergetic killing roles with radiation in the multi-drug resistant SKVCR ovarian cancer cells. *Radiat Oncol*. 2012;7:213.
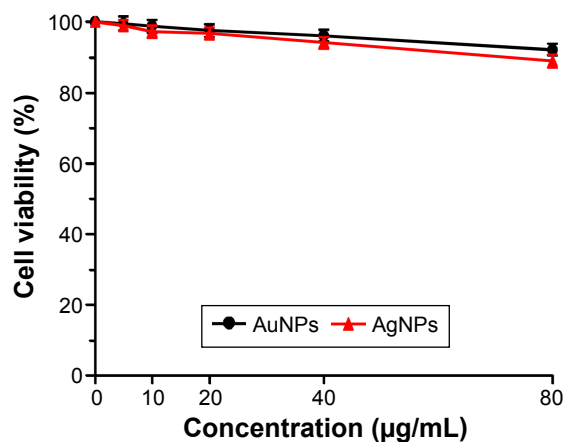
Supplementary materials

Figure S1 Cytotoxicity of AuNPs and AgNPs on 184B5 human mammary epithelial cells.

Notes: The cell viability was determined using a CCK-8 assay after a 24-hour exposure of AuNPs or AgNPs at multiple concentrations. Data are a summary of three independent experiments and expressed as mean ± SD.

Abbreviations: AgNPs, silver nanoparticles; AuNPs, gold nanoparticles; CCK-8, Cell Counting Kit-8; SD, standard deviation.
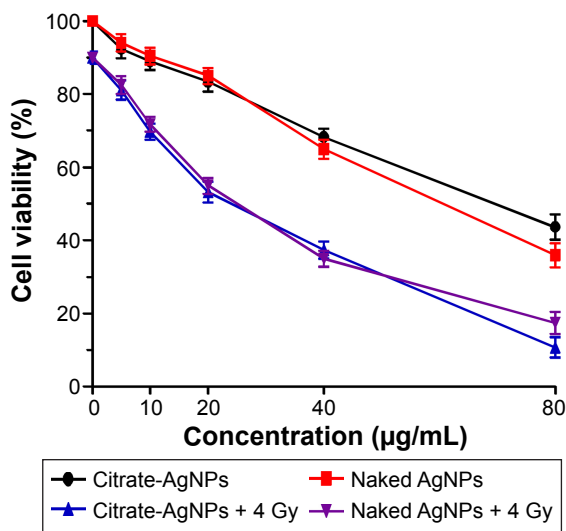

Figure S3 Effects of AuNPs and AgNPs plus radiation on 184B5 epithelial cell viability.

Notes: Cells were incubated for 24 hours with 10 μg/mL AuNPs or AgNPs. At 24 hours after radiation treatment, the cell viability was determined using a CCK-8 assay. Data are a summary of three independent experiments and expressed as mean ± SD.

Abbreviations: AgNPs, silver nanoparticles; AuNPs, gold nanoparticles; CCK-8, Cell Counting Kit-8; SD, standard deviation.

Figure S2 Effects of citrate-coated and naked AgNPs on U251 glioma cell viability with or without radiation.

Notes: Cells were incubated for 24 hours with varying concentrations of AgNPs. At 24 hours after radiation treatment, the cell viability was determined using a CCK-8 assay. Data are a summary of three independent experiments and expressed as mean ± SD.

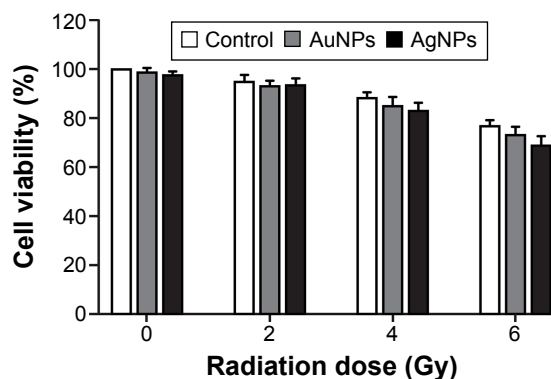**Abbreviations:** AgNPs, silver nanoparticles; CCK-8, Cell Counting Kit-8; SD, standard deviation.